

OMAE2008-57247

APPLICATION OF LINEARIZED MORISON LOAD IN PIPE LAY STINGER DESIGN

Riaan van 't Veer

GustoMSC

Hydrodynamic and Stability Department
Schiedam, The Netherlands

ABSTRACT

This paper presents numerical results of ship motions and global stinger loads through a combined hydrodynamic analysis of a pipe lay vessel with submerged stinger. The results of nonlinear time domain simulations are compared to those obtained through linearization of the Morison load on the slender stinger elements. Through linearization, an iterative frequency domain solution scheme is developed reducing analysis time significantly. Response amplitude operators in operating and limiting sea states are shown, including the influence of current velocity. Through nonlinear time domain simulations insight is obtained on the distribution and magnitude of the extreme values.

KEYWORDS

Morison load, Stochastic linearization, Pipe lay vessel

INTRODUCTION

The structural design of a submerged stinger for pipe lay operation is part of a complex design loop. The hydrodynamic loads on the slender elements of the stinger result in global loads at the hinges where the stinger connects to the ship. Apart from these global structural loads, each member of the stinger is subject to line loads. In an optimized design, the pipe diameter and wall thickness of the tubes are designed to withstand these local structural loads given certain structural allowances. Other design constraints can be the stinger handling, structural integration of the stinger in the aft ship, and obviously steel production costs. This paper will focus on a fast calculation method to derive global stinger loads by means of combined ship-stinger motion analyses.

During pipe lay operation the heading of the ship can not be chosen, thus the operational profile includes all possible wave headings. If the wave environment becomes too harsh, which is generally so above 4 m significant wave height, the stinger might be retrieved out of the water. In such a situation the stinger is temporarily located in the splash zone. As a result

the wave loads might be very significant for short duration of time. If the stinger is rigidly connected to the vessel and can not be taken out of the water, wave loads might be minimized by abandoning the pipe and by taking sheltered heading. But it is not on forehand clear at which heading global stinger loads reach a minimum if the heading can be selected.

The above sketches the complexity in the design phase, which consists of, among other factors: a large series of possible environmental combinations of waves, wind and current, and a complex hydrodynamic ship-stinger interaction with possible multiple stinger orientations.

STINGER DESIGN LOOP

An initial stinger design starts with an OFFPIPE run to establish the overall dimensions of the stinger. Based on experience, a first design of a lattice stinger structure is made. A following step is to establish the structural loads due to ship motions. Depending on the stinger dimensions and orientation of the stinger in the water, the drag and inertia loads on the stinger elements will influence the ship motions to more or less extent. Since the pipe lay vessel cannot change its heading during pipe lay operation, the ship-stinger motions and resulting structural loads need to be assessed for all possible headings, a collection of operational and limiting sea states, and if an adjustable stinger is designed, for several stinger curvatures. To optimize the stinger design, the above sketched procedure is repeated iteratively until the structural load distribution on the stinger matches the design requirements.

The stinger and the ship are interaction structures. Ship motions are most efficiently solved in the linear frequency domain, and now-a-days a diffraction panel method has become the standard to do so. However, the hydrodynamic loads on the slender stinger elements, due to current, waves and ship motions, follow from Morison's equation. This equation describes the loads in terms of a nonlinear drag force and linear inertia force perpendicular to the principal axis of the element.

The nonlinear drag term prohibits direct application of the Morison's equation in linear frequency domain.

To account correctly for the nonlinear drag loads on the stinger elements, a time domain solver including Morison element modeling is required. Such simulation programs are widely available; an example is the ANSYS-AQWA suite of programs. But application of a nonlinear time domain solver in the early 'iterative' design stage is not preferred, due to the significant analysis time involved for each load case. Fast frequency domain calculations are preferred.

The linearization approach and its application is the topic of the present paper. In view of the large number of varying parameters, the application is already useful when the worst sea states can be found, and even more if a good estimate of the hinge loads is obtained. But, it is expected that in those conditions where the stinger damping dominates the motion equations, nonlinear time domain simulations are needed to obtain accurate design extremes given a typical storm duration.

SHIP-STINGER INTEGRATION

The ship and stinger are defined as two separate structures. This paper presents the results for a fixed stinger only, in other words a stinger that is rigidly connected to the ship. The ship is considered as a diffracting body. The slender elements of the stinger are only subject to drag and inertia loads, described as Morison loads. The velocities and accelerations in that formulation are due to the combined effect of ship motions, current and sea state.

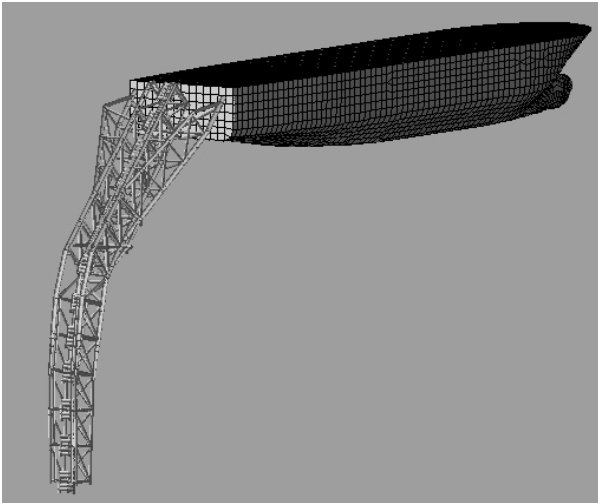


Figure 1: Ship with Stinger, AQWA modelling

The stinger and ship configuration as presented in Figure 1 defines the configuration. Global hinge loads are calculated in a point where stinger attaches to the ship.

MOTION EQUATION

The motion equation for a floating structure with attached stinger can be written, in the time domain, as:

$$\mathbf{M}\ddot{\xi}(t) = \vec{F}_{SHIP}(t) + \vec{F}_{STINGER}(t) \quad (1)$$

where $\vec{F}_{SHIP}(t)$ represents the hydrodynamic forces on the vessel, $\vec{F}_{STINGER}(t)$ represents the Morison load on slender stinger elements. The mass matrix of the total system is defined by \mathbf{M} . The accelerations $\ddot{\xi}(t)$ are solved in a time stepping procedure, and the motions $\xi(t)$ follow from integration. If the stinger is rigidly connected to the vessel, the motion vector $\xi(t)$ contains six rigid body motion components. The Morison load on slender (tubular) elements is given by:

$$\vec{F}_{STINGER}(t) = \frac{1}{2}\rho DC_D \vec{u}(t) |\vec{u}(t)| + \frac{\pi}{4}\rho D^2 C_M \dot{\vec{u}}(t) \quad (2)$$

where $\vec{u}(t)$ is the flow velocity experienced by the element and $\dot{\vec{u}}(t)$ the acceleration. The drag and inertia coefficients are given by C_D and C_M respectively.

Equation (1) can be solved in time domain using the ANSYS-AQWA software. The Morison load on submerged slender stinger elements are modeled as in equation (2). To solve equation (1) in the frequency domain, all terms are to be expressed as harmonic varying signals with constant amplitude, which means that equation (2) needs to be linearized. In the frequency domain approach the motion equations are solved for a series of regular waves which sum up to the wave spectrum. A similar breakdown is the basis of time domain simulations where the motion equations are solved in a time-stepping approach.

LOADS ON SUBMERGED STINGER ELEMENTS

The forces (per unit length) on submerged slender tubular elements are described by the Morison equation, which in relative-velocity expression read as:

$$\begin{aligned} \vec{F}(t) &= \frac{1}{2}\rho DC_D |\vec{u}| \vec{u} + \frac{\pi}{4}\rho D^2 C_M \dot{\vec{u}} \\ &= \frac{1}{2}\rho DC_D |\vec{u}_c + \vec{u}_w - \dot{\vec{x}}| (\vec{u}_c + \vec{u}_w - \dot{\vec{x}}) \\ &\quad + \frac{\pi}{4}\rho D^2 C_M \dot{\vec{u}}_w - \frac{\pi}{4}\rho D^2 C_A \ddot{\vec{x}} \end{aligned} \quad (3)$$

The velocity field around an element is the result of a constant current velocity, \vec{u}_c , varying wave orbital velocities $\vec{u}_w(\vec{x}, t)$ and varying element motions $\dot{\vec{x}}(\vec{x}, t)$. The drag coefficient C_D

is constant in time as well as the mass inertia coefficient C_M ; the added mass coefficient is related to the mass inertia coefficient as $C_M = 1 + C_A$.

As often mentioned, the Morison equation with constant coefficients is an approximated solution to a complex problem. The complexity lies in the varying flow field around slender elements, which is viscous dominated. Typical non-dimensional parameters to identify the flow field around an oscillating object are the Reynolds (Re) and Keulegan-Carpenter (KC) number. Due to the complex lattice structure of the stinger and associated flow field around it, Re and KC numbers will vary along the stinger from sea state to sea state. Significant interaction effects between members are expected but experimental data is scarce to non-existing for stinger constructions. And even then, model tests determining the flow field or forces on the stinger will be subject to important model scale effects, so the extrapolation to full scale remains difficult.

Originally, Morison's equation was postulated for forces on fixed slender elements, thus without member motion. Research on the applicability of the combined flow field, see for example Shafiee-Far [1], shows that the relative velocity formulation gives adequate results for oscillating members in current and waves.

The main concern of this paper is to demonstrate a working procedure to verify if a linearized Morison equation in a frequency domain calculation suffices to determine design load cases. In view of the purpose of this paper the drag and inertia coefficients are considered equal for all stinger elements. Based on an estimate of the Re and KC numbers and expected stinger element smoothness, a drag coefficient of $C_D = 1.05$ and an inertia coefficient of $C_M = 0.8$ are selected as representative.

LINEARIZED MOTION EQUATIONS

To account for the drag loads in a frequency domain approach, equation (2) is written in a generic linear form:

$$\bar{F}_{LIN}(t) = \frac{1}{2} \rho D \bar{C}_D u + \frac{\pi}{4} \rho D^2 C_M \dot{u} \quad (4)$$

A common approach is to calculate the linearized drag term \bar{C}_D from equating the energy dissipation from the linear and nonlinear drag contribution (equivalent linearization), or by minimizing the error between the linear and nonlinear force (stochastic linearization). Details of the two approaches are described below.

When the velocity variation are sinusoidal with constant amplitude - like in regular waves - thus $u(t) = u_a \cos(\omega t)$, the linearized force is given by:

$$F(t) = \frac{1}{2} \rho D C_D [8 / (3\pi) u_a] \cdot u \approx \frac{1}{2} \rho D C_D [1.2004 \sigma_u] \cdot u \quad (5)$$

where σ_u is the standard deviation of the regular sinusoidal velocity ($\sigma_u = u_a / \sqrt{2}$). The linearization factor between square brackets is obtained from equating the energy in a quarter of the oscillation period, that is:

$$\int_0^{T/4} (C_D u |u|) u dt = \int_0^{T/4} (\bar{C}_D u) u dt \quad (6)$$

Linearization of the force due to a random oscillatory velocity - like in irregular waves - leads to, see for example Borgman [2] or Wolfram [4]:

$$F(t) = \frac{1}{2} \rho D C_D u \sqrt{(8/\pi) \sigma_u} \approx \frac{1}{2} \rho D C_D [1.596 \sigma_u] \cdot u \quad (7)$$

where σ_u is the standard deviation of the velocity spectrum and $u(t)$ the random velocity time trace. The last linearization procedure is denoted stochastic linearization. The linearization factor in an irregular (Gaussian) sea state is obtained from minimizing the time averaged least square error between the linear, $F_{LIN}(t)$, and nonlinear time signal $F(t)$, as in [4]:

$$\frac{\partial \langle (F_{LIN}(t) - F(t))^2 \rangle}{\partial \bar{C}_D} = -2 \langle \bar{C}_D u^2 |u| - C_D u^2 \rangle = 0 \quad (8)$$

where $\langle \rangle$ indicates the expected (time-averaged) value. If the wave elevation is assumed to follow a Gaussian distribution, the derived velocity field and all calculated linear responses follow a Gaussian distribution as well and equation (7) applies.

Both approaches assume a zero mean signal, thus a zero current velocity. Along the stinger the ratio between the wave orbital velocity and motion induced velocity depends very much on the location of the element. The motion induced velocities at the tip of the stinger will be much larger than near the stinger hinge. Including current complicates direct insight in the relative importance of the different velocity components. An approximation of the time varying drag contribution with current is obtained from applying the triangle inequality, leading to:

$$F(t) = 0.5 \rho D C_D \left[2 |u_c| + \sqrt{(8/\pi) \sigma_{u_w - \dot{x}}} \right] (u_w - \dot{x}) \quad (9)$$

Note that the current velocity occurs only in the linearization term, so that equation (9) can be applied in a frequency domain approach.

The outline above shows that stochastic linearization does not converge to the equivalent linearization when the sea state consists of a single wave component. As such, one could argue that equivalent linearization is a valid approach in a sea state since that is constructed from a series of regular waves and motion equations are solved for each regular wave separately. And even in time domain the basis is regular wave summation and most forces are defined based on this. Comparing both approaches to nonlinear time domain results will reveal the validity of the methods.

As shown by several authors, like Brouwers [3] and Wolfram [4], the linearized Morison equation under predicts the extreme peaks compared to the nonlinear equation. For a moving stinger the motion extremes are thus most likely over predicted. The affect on the hinge loads could be large. Brouwers [3] defines a correction factor (3 h extreme over standard deviation) for fatigue load depending on the drag versus inertia ratio which becomes as large as 8 for drag dominated structures.

In view of the above discussion, application of the linearized Morison's equation is useful when it provides the initial load level for all possible environmental conditions. The absolute load level and accurate extreme value prediction can most likely only obtained using the nonlinear Morison equation directly in time domain simulations. As quoted from Wolfram [4]: 'In some cases it may be more expedient to solve the nonlinear equation numerically than to bother with linearization'.

IMPLEMENTATION IN FREQUENCY DOMAIN

The linearized frequency domain solution including linear Morison loads is solved iteratively. The linearization factor is calculated for each stinger element, based on the standard deviation of the relative velocity on that element from the previous iteration. The overall ship motion components are used to calculate that local member velocity. The spectrum is constructed from a summation of regular waves and for each regular wave the motion equations are solved.

Conceptually, the equivalent linearization uses the standard deviation of the velocity at the element calculated for each wave frequency. Thus for each beam and for each wave frequency, σ_u is related to the velocity amplitude on the element in a regular wave which amplitude corresponds to the spectral density distribution. Stochastic linearization calculates the standard deviation from the velocity spectrum found for each beam using all frequencies, that is $\sigma_u = \sqrt{m_{0,u}}$. The motion equations for each frequency apply this factor.

For each stinger element a transformation matrix \mathbf{T}_G^L is defined which is used to calculate the contribution of the element to the global force $\vec{F}_{MORISON}$ from the local Morison force \vec{F}_L (perpendicular to the element orientation):

$$\vec{F}_{MORISON,G} = \sum_{i=1}^N \mathbf{T}_{G,i}^L \vec{F}_{L,i} \quad (10)$$

For convenience a skew-matrix $\mathbf{S}(\vec{r})$ is defined which comprises the location of the stinger with respect to the global frame of reference. The indices i are left out to shorten notation:

$$\mathbf{S}(\vec{r}) = \begin{bmatrix} 0 & -z & y \\ z & 0 & -x \\ -y & x & 0 \end{bmatrix} \quad (11)$$

The tube CoG is located at \vec{r} from the global origin, so its acceleration in the global frame of reference is:

$$\ddot{\vec{x}} = \ddot{\vec{x}}_{COG} + \dot{\vec{\omega}} \times \vec{r} = \ddot{\vec{x}}_{COG} - \mathbf{S}(\vec{r}) \dot{\vec{\omega}} \quad (12)$$

where $\vec{\omega}$ is the ship rotational velocity. The accelerations in the local frame are then:

$$\ddot{\vec{x}}_L = \mathbf{T}_L^G \ddot{\vec{x}}_G \quad (13)$$

so that it is possible to write:

$$\vec{F}_G = -\mathbf{T}_G^L \mathbf{M}_{C_A} \mathbf{T}_L^G \left\{ \ddot{\vec{x}} - \mathbf{S}(\vec{r}) \dot{\vec{\omega}} \right\} \quad (14)$$

where \mathbf{M} is the mass matrix of the local element, in which the inertia of the tube around its own axis system is neglected:

$$\mathbf{M}_{TUBE} = \begin{bmatrix} m \mathbf{I}_{3 \times 3} & -m \mathbf{S}(\vec{r}) \\ m \mathbf{S}(\vec{r}) & -m \mathbf{S}(\vec{r}) \mathbf{S}(\vec{r}) \end{bmatrix} \quad (15)$$

Using the above derivations, the inertia force of a single element of the stinger can now be written as:

$$\begin{bmatrix} \vec{F} \\ \vec{M} \end{bmatrix}_G = - \begin{bmatrix} \mathbf{T}_G^L \mathbf{M}_{C_A} \mathbf{T}_L^G & 0 \\ \mathbf{S}(\vec{r}) \mathbf{T}_G^L \mathbf{M}_{C_A} \mathbf{T}_L^G & 0 \end{bmatrix} \begin{bmatrix} \mathbf{I}_{3 \times 3} & -\mathbf{S}(\vec{r}) \\ \mathbf{I}_{3 \times 3} & -\mathbf{S}(\vec{r}) \end{bmatrix} \begin{bmatrix} \ddot{\vec{x}} \\ \dot{\vec{\omega}} \end{bmatrix}_G \quad (16)$$

A similar expression can be derived for the linearized drag term, leading to:

$$\begin{bmatrix} \vec{F} \\ \vec{M} \end{bmatrix}_G = \begin{bmatrix} \mathbf{T}_G^L \mathbf{B}_{C_D} \mathbf{T}_L^G & 0 \\ \mathbf{S}(\vec{r}) \mathbf{T}_G^L \mathbf{B}_{C_D} \mathbf{T}_L^G & 0 \end{bmatrix} \begin{bmatrix} \mathbf{I}_{3 \times 3} & -\mathbf{S}(\vec{r}) \\ \mathbf{I}_{3 \times 3} & -\mathbf{S}(\vec{r}) \end{bmatrix} \begin{bmatrix} \dot{\vec{x}} \\ \dot{\vec{\omega}} \end{bmatrix} \quad (17)$$

The linearization factor is included in the damping matrix \mathbf{B}_{C_D} .

This matrix includes the standard deviation of the local velocity, as expressed in equations (5) and (7).

The wave excitation forces and moments due to wave orbital acceleration $\dot{\vec{u}}_w$ acting on the elements is given by:

$$\begin{aligned} \vec{F} &= [\mathbf{T}_L^G \mathbf{M}_{C_M} \mathbf{T}_G^L] \dot{\vec{u}}_w \\ \vec{M} &= \mathbf{S}(\vec{r}) \vec{F} \end{aligned} \quad (18)$$

The water orbital velocities on each stinger element are evaluated in the midpoint of each element, and in agreement with linear frequency theory, at the location when the ship is at rest.

TIME DOMAIN SIMULATIONS

The AQWA software is used to perform the time domain simulations. The Morison elements apply the relative velocity formulation. This is part of the software already, so no additional ad-hoc modeling is required. A 2-point Gaussian quadrature rule is used to calculate the relative velocity and acceleration on each element. The drag and inertia coefficients of each element are pre-defined and constant during a simulation. The location of a slender Morison element with respect to the actual water line is evaluated and used to determine the time dependent Morison load. The AQWA-NAUT module accounts for nonlinear stiffness and wave forces on diffracting bodies as well. The linear potential damping from the frequency domain is used to calculate the convolution integrals. The retardation forces are calculated using these integrals with the appropriate time history signals. A mixed approach is thus used, linear convolution integrals with the actual ship motion velocities which include possible nonlinear effects due to nonlinear force components in the model. The Morison drag and the ship stiffness and wave excitation forces are the nonlinear components. To avoid a drifting model, a spread-mooring system with appropriate stiffness and pre-tensioning is used. This kind of modeling compares with a model basin set-up.

APPLICATION

The ship-stinger configuration as shown in Figure 1 is used throughout this paper. The ship motions are first calculated in the frequency domain, without the stinger. In addition to the hull surface mesh, an internal free surface mesh is applied to suppress possible irregular frequencies that can lead to inaccurate convolution integrals for the time domain solver. The ship has overall dimensions of about 145 m length and 21 m

beam. Recently GustoMSC was involved in the vessel upgrade, design of the ship-stinger integration and stinger handling frame. For this purpose, the integral assessment of the stinger and vessel motions was carried out, including an assessment of the hinge loads in operational and survival sea states.

In that project, pipe lay conditions include sea states up to 2 m significant wave height with associated wind conditions. Since the ship can not freely choose its heading during pipe lay, all possible headings are to be considered. Above 2 m significant pipe lay operation is abandoned. In those conditions the vessel is assumed capable to select its heading, so that roll motions and stinger loads can be minimized. To avoid even larger hydrodynamic stinger loads, the stinger is taken out of the water above 4 m significant wave height by the stinger handling frame. Current velocities are considered up to 2 knots with uncorrelated direction with respect to the sea state.

The stinger orientation and curvature is adjustable depending on the type of pipe diameter and pipe laying water depth. All results in this paper assume deep water, but it is not a restriction in AQWA. The stinger is about 70 m long consisting of 1002 different tubular elements. Smaller elements are neglected, as well as non-tubular elements in the rollerboxes, walkways above main stinger tubes and others. To account for the drag and inertia of these and neglected construction details, drag and inertia values of selected members are corrected.

The stinger and the ship are defined as two individual structures in AQWA. A single hinge point with zero degree of freedom is used at which both structures connect. The intersection loads are then directly obtained in time domain. The ship is the only diffracting body. The potential added mass, damping, diffraction and Froude-Kryloff forces on the ship are calculated in the frequency domain. The location of the centre of gravity of the ship is defined such that the overall ship-stinger combination centre of buoyancy (CoB) and centre of gravity (CoG) are vertically in-line resulting in zero trim. The mass of the ship is corrected for the stinger mass being 3.2% of the ship mass. Since only the frequency domain coefficients are used in post-processing, discrepancy between the vertical alignment of the ship CoB and CoG in the frequency domain is of no influence.

COMPARISON BETWEEN EQUIVALENT AND STOCHASTIC LINEARIZATION

In Figure 2 the roll RAO in beam seas obtained through equivalent and stochastic linearization is given, without and with 2 m/s current (sea state aligned). The result is obtained in a JONSWAP sea state with $H_s = 2$ m, $T_p = 13$ s and $\gamma = 3.3$. The torsion moment M_X at the stinger hinge is presented in Figure 3.

As the results show, both methods predict comparable motion and load responses. The roll motion peak is slightly higher when using stochastic linearization. The impact of this

on the roll moment is small. The verification was made for other motion and load components, showing comparable trends.

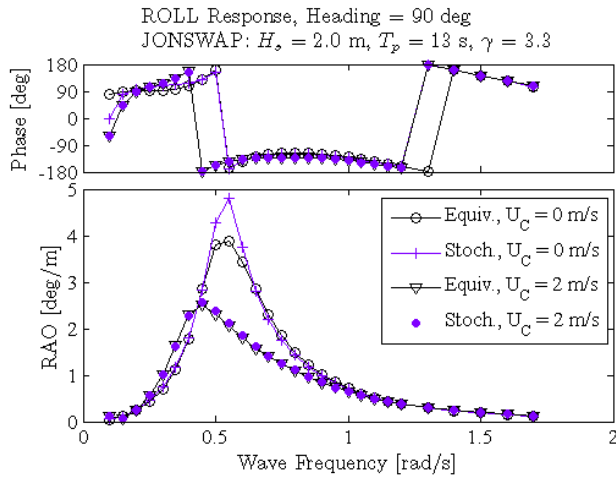


Figure 2: Comparison of Roll motion RAO in beam seas using different linearization approaches.

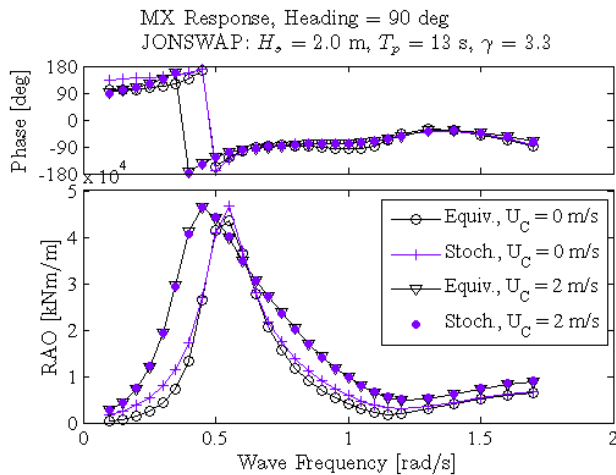


Figure 3: Comparison of Load MX RAO in beam seas using different linearization approaches.

SHIP-STINGER MOTIONS IN BEAM SEAS

In Figure 4 through Figure 7 a comparison is given of the sway, heave, roll and pitch response amplitude operators (RAOs) with phase, in beam seas, using different calculation methods.

The linear frequency domain calculations, denoted ‘FD, Ship only’ in the figures, apply a fixed additional damping to correct for the bilge keel damping. At the natural peak the roll damping is 8% of the critical damping. AQWA has no implementation of an empirical roll damping method in frequency domain. The results with stinger damping are denoted ‘FD, Ship + Stinger, Equiv’ when iteratively obtained in a

spectrum decomposition with equivalent damping, and ‘FD, Ship + Stinger, Stoch’, when iteratively obtained in a spectrum decomposition with stochastic linearization. The time domain simulations are performed with AQWA-NAUT in the given spectrum with nonlinear Morison loads for a duration of 3-hours, and the RAO is retrieved from time trace post-processing.

The results show that the stinger adds significant damping, reducing roll and pitch motion amplitudes. Sway and heave are marginally if at all influenced at this heading. The natural roll period of the ship with stinger reduces and the shift is well predicted by stochastic linearization. Equivalent linearization slightly under predict the peak roll response. But basically, all motion components are well predicted by both linearization methods compared to the nonlinear time domain simulation result.

Figure 8 presents the distribution of the absolute value of the roll amplitudes based on 9-hour time domain simulation data. The current of 1 m/s aligns with the waves. The results indicate that the roll crest and troughs are not Rayleigh distributed while the sea state in the simulations is Gaussian distributed. This could be expected since the damping of the stinger is nonlinear and adds in particular to the roll damping. The given Weibull and Rayleigh fit is performed on all simulated crest and through extreme data points with zero current speed. As can be seen, the current velocity in itself has a significant influence on the distribution as well but, in this example, less on the extreme values near the tail of the distribution.

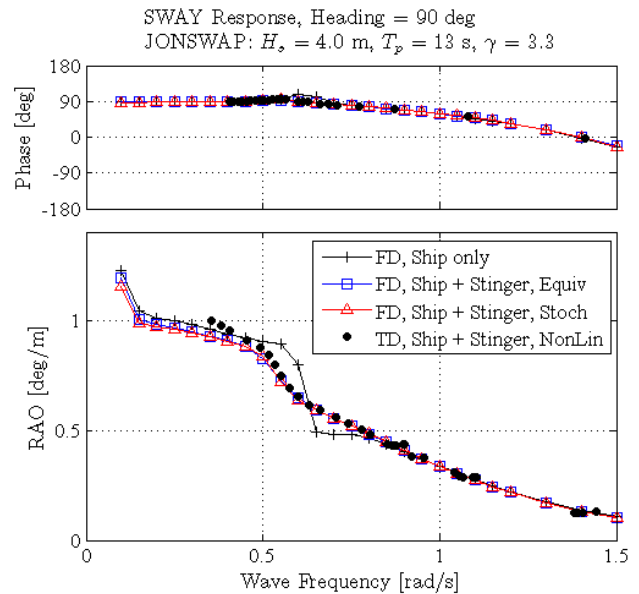


Figure 4: Sway response in beam seas.

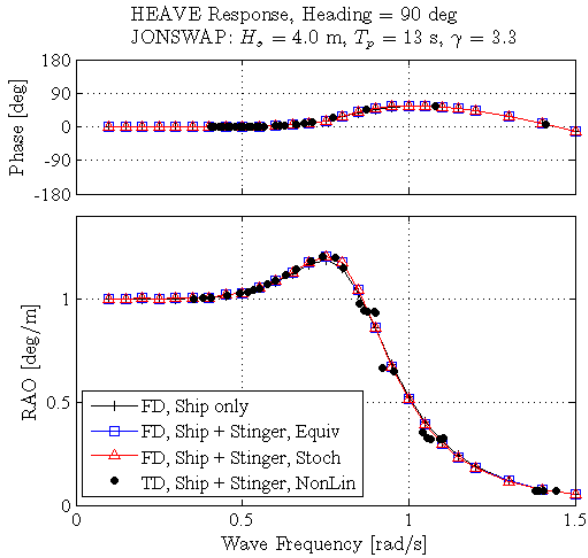


Figure 5: Heave response in beam seas

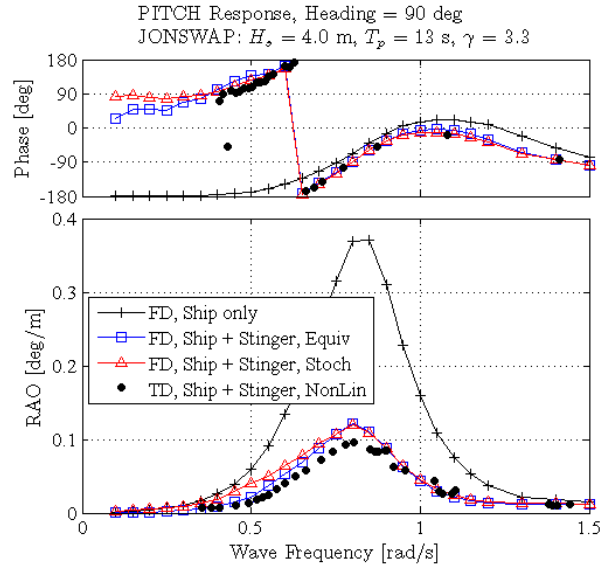


Figure 7: Pitch response in beam seas

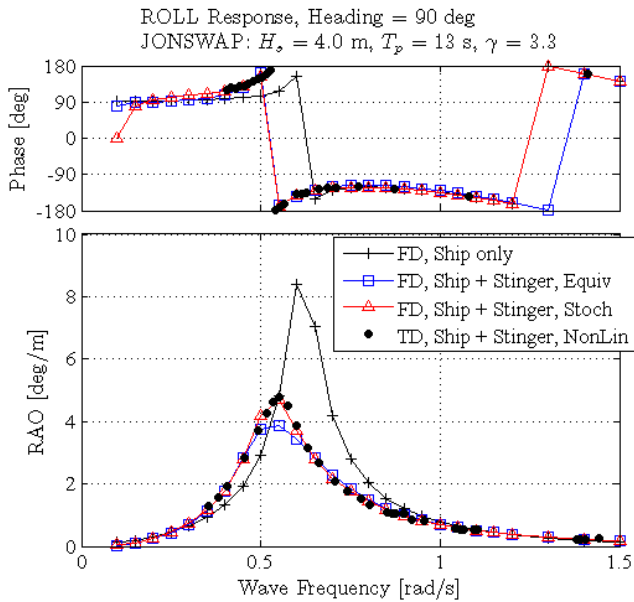


Figure 6: Roll response in beam seas

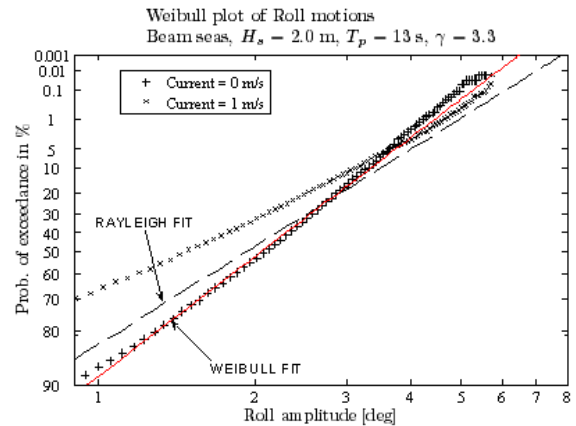


Figure 8: Distribution of Roll crest and troughs in $H_s = 2$ m from nonlinear time domain simulations

STINGER HINGE LOADS

In Figure 9 the distribution of positive roll moment M_x crests in the hinge are given for the same two conditions as the roll motions of Figure 8. A two parameter Weibull fit on all data points gives a good prediction for the extremes. The results show that a 3-hour extreme M_x moment would be under predicted using a Rayleigh distribution.

In the early design stage the absolute value prediction for the hinge loads is important, but even more important is to find the correct load trend with respect to the parameters involved, like heading, sea state and current velocity. If the most severe conditions can be located, a few time domain simulations for these conditions using an already optimized design are not

extremely time consuming in terms of CPU time or problem modeling. Such simulations will reveal the actual load level and can be used to obtain the distributions to predict the extreme values given a probability of exceedance.

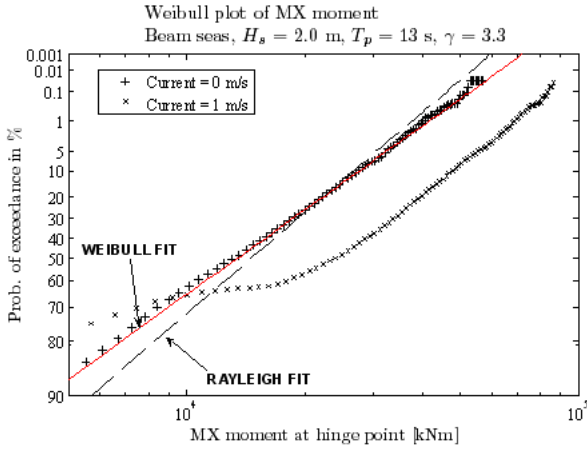


Figure 9: Distribution of MX at stinger hinge in $H_s = 2$ m from nonlinear time domain simulations

Figure 10 through Figure 15 show the load RAO at the hinge point in bow quartering seas of $H_s = 2$ m, with and without current in bow quartering seas (heading 150 deg). In general the RAO obtained from stochastic linearized calculations in frequency domain compare well with those obtained from the nonlinear time domain. Where discrepancies are the largest, that is for the M_x and M_z moment, the frequency domain results over predict the RAO, and are thus conservative. The trend with increasing current velocity is very well predicted.

A comparison of the standard deviation in the JONSWAP spectrum with $H_s = 2$ m and $T_p = 13$ s is given in Table 1. Apart from roll moment M_x the standard deviation from the stochastic linearized calculations and time domain simulation (using all data samples) compares well. The table also presents the 3-hour extreme value from the time trace and the corresponding factor between standard deviation and the 3 hour extreme. The factors obtained are between 3.3 and 7.8 while linear theory would predict a factor of about $2 \cdot 1.86 = 3.7$. This indicates that by assuming a Gaussian/Rayleigh stochastic process, the 3 hours most probable hinge load extreme will be under predicted. This confirms the findings in Brouwers [3] who present a factor for the expected extreme with respect to the standard deviation, which increases from 3.7 for (linear) inertia dominated systems to as large as 8 when drag dominates the load.

Table 1: Comparison of extreme value prediction

JONSWAP, $H_s = 2$ m, $T_p = 13$ s, $\gamma = 3.3$; Heading = 150 deg						
	FX [kN]	FY [kN]	FZ [kN]	MX [kNm]	MY [kNm]	MZ [kNm]
Time domain simulation						
mean			-5576		-151 10^3	
st. dev	266	193	343	5975	18195	6537
+ max 3h	2071	746	-3891	24 10^3	-53 10^3	29 10^3
- max 3h	-1572	-943	-7055	-26 10^3	-285 10^3	-21 10^3
expected	7.8	3.9	4.9	4.0	5.4	4.6
extreme / st. dev	5.9	4.9	4.3	4.4	7.4	3.3
Frequency domain with stochastic linearization						
mean			-5427		-154.8	
st. dev	209	197	375	9303	16102	6578

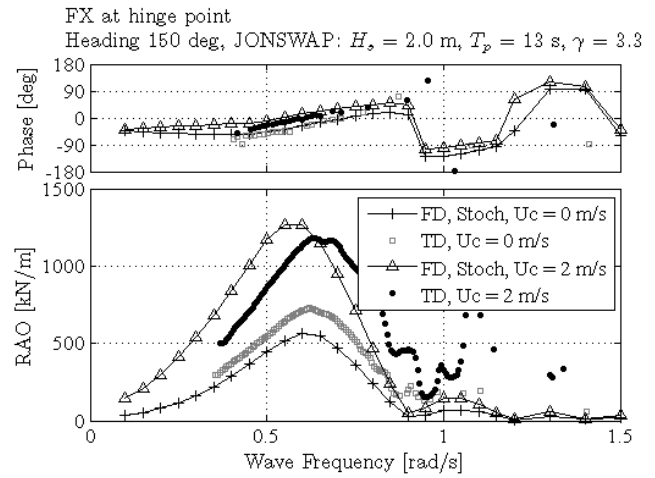


Figure 10: FX hinge load RAO in bow quartering seas

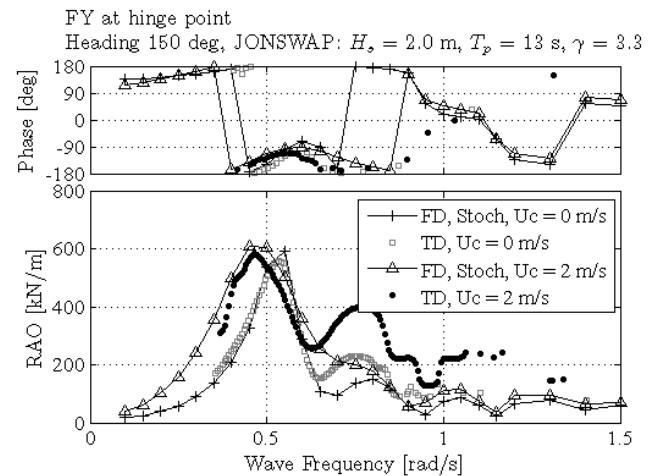


Figure 11: FY hinge load RAO in bow quartering seas

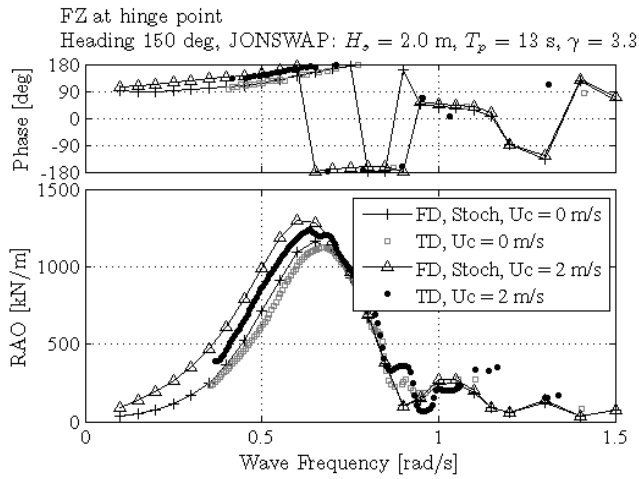


Figure 12: FZ hinge load in bow quartering seas

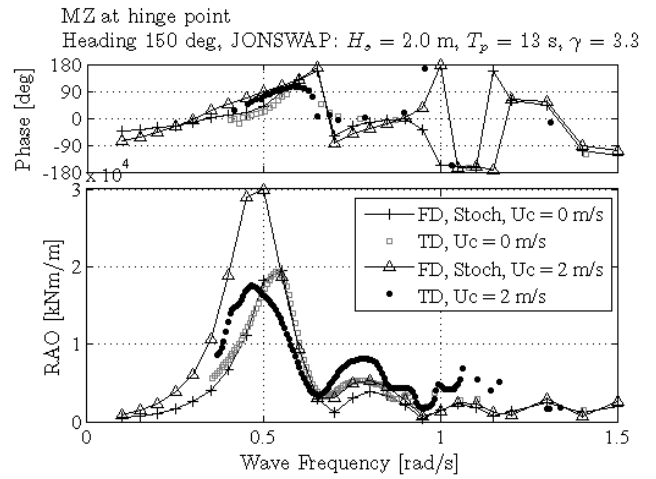


Figure 15: MZ hinge load in bow quartering seas

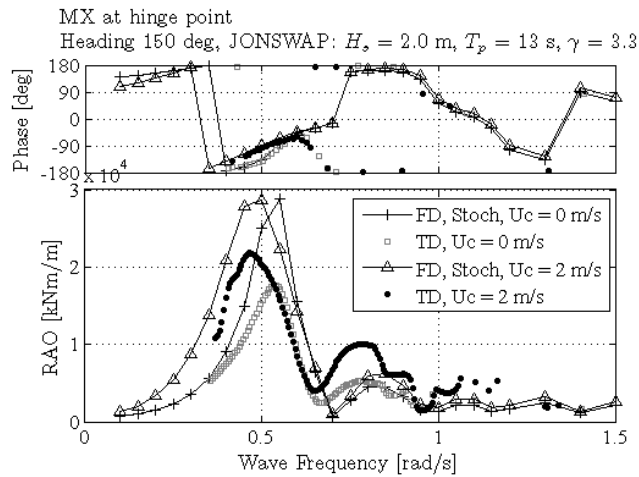


Figure 13: MX hinge load in bow quartering seas

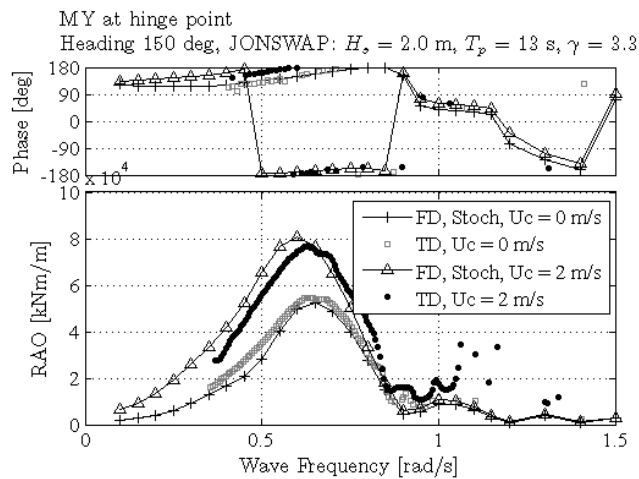


Figure 14: MY hinge load in bow quartering seas

INFLUENCE OF HEADING

The standard deviation of the motions and loads is calculated for every 10 deg heading variation in an operational sea state. Current velocity is 0 m/s. The comparison between stochastic linearized frequency domain and nonlinear time domain are presented in Figure 16 for the 6 DOF ship motions and in Figure 17 for the global hinge loads.

The results show good correlation and demonstrate that the linearized approach can be used to locate the worst case conditions and can provide a first initial design load. The fact that the F_y load level is very well predicted and the M_x load to lesser extends indicates that the distribution of load over the members is somewhat different in time domain simulations.

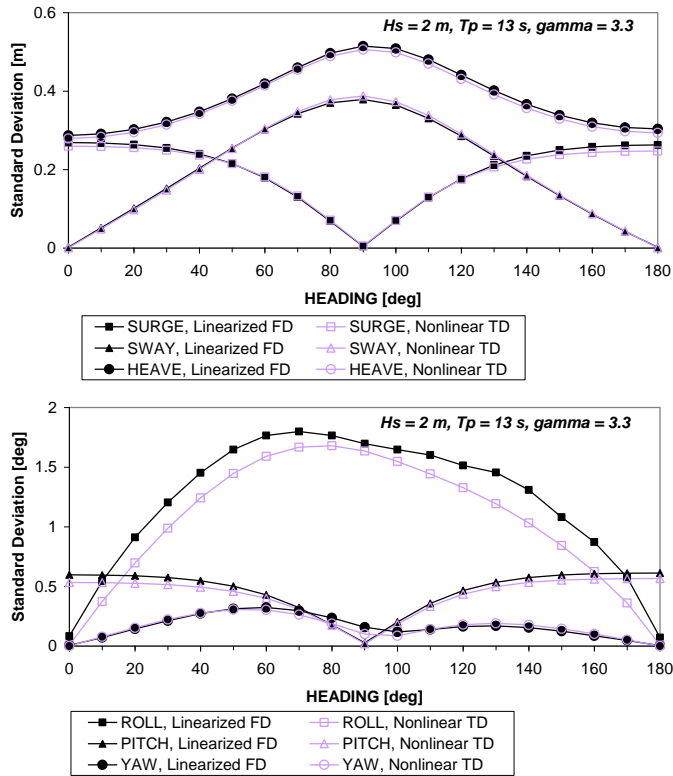


Figure 16: Standard deviation of ship motions

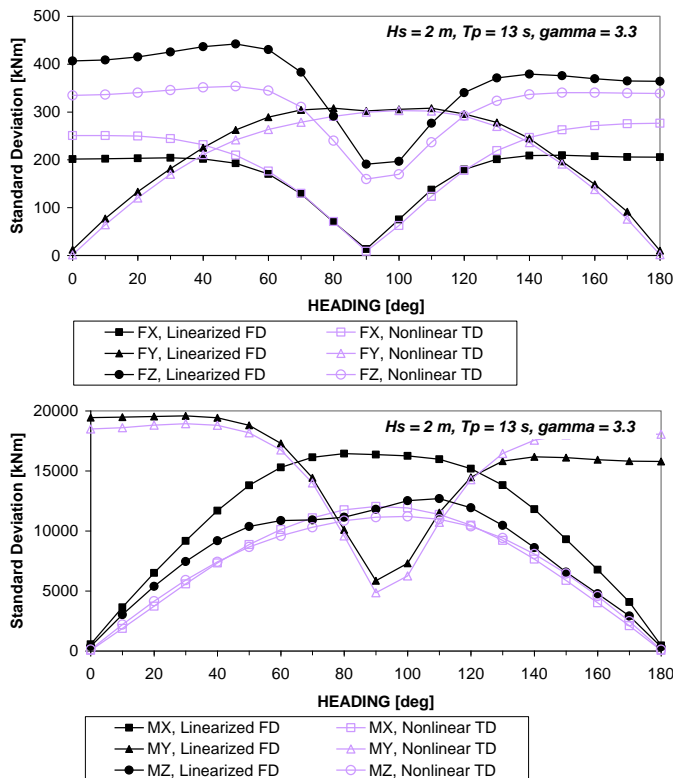


Figure 17: Standard deviation of hinge loads

CONCLUSIONS

The Morison load on a stinger is linearized using an equivalent and stochastic approach. Both methods are applied in an iterative frequency domain solver, which typically converges in less than 10 iterations. Stochastic linearization is considered more applicable in a sea state, but both methods perform well.

The overall ship motions and global stinger hinge load response amplitude operators from linearized calculations are compared with those obtained from nonlinear time domain simulations, showing good correlation. The influence of wave height and current is well captured. It is further shown that the distribution of extremes from a time domain simulation do not follow the Rayleigh distribution, which was expected since the transfer is nonlinear due to the Morison drag loads. The ratio between the most probable 3 hour extreme and standard deviation obtained from time domain simulations is found to vary from 3.3 to 7.8, while it is generally around 5, which indicate that linearized theory assuming a Gaussian process transfer (leading to a factor of 3.7) will under predict the global hinge loads, even if the standard deviation is well predicted.

It is shown that application of linearized Morison load in pipe lay design can locate the worst sea state conditions, including the influence of current. Nonlinear time domain simulations remain required to obtain the correct design load level.

REFERENCES

- [1] Shafiee-Far, M. (1997): Hydrodynamic interaction between fluid flow and oscillating slender cylinders. PhD thesis, Delft University of Technology
- [2] Borgman, L.E. (1967): Random Hydrodynamic Forces on Objects, Annals of Mathematical Statistics, pp. 37-51
- [3] Brouwers, J.J.H, and Verbeek, P.H.J (1983): Expected fatigue damage and expected extreme response for Morison-type wave loading, Applied Ocean Research, Vol 5, No. 3, pp 129-133
- [4] Wolfram, J. (1998): On alternative approaches to linearization and Morison's equation for wave forces, Proc. R. Soc. London, Vol. 455, pp. 2957-2974